



High power nanosecond optical vortex laser oscillation in mode-selection slab resonator

Tian-Li Yang^{1,2} · Jing Yang¹ · Xue-Peng Li¹ · Hao Wang^{1,2} · Zong-Zhe Zhang¹ · Yun-Ping Wang³ · Xiao-Jun Wang¹

Received: 28 February 2024 / Accepted: 1 May 2024 / Published online: 11 May 2024
© The Author(s), under exclusive licence to Springer-Verlag GmbH Germany, part of Springer Nature 2024

Abstract

A method for generating high-power, millijoule level single pulse energy optical vortex laser using a mode-selection slab resonator is proposed and experimentally demonstrated. The optical resonator forms a stable cavity with just two mirrors and a Nd: YAG laser slab, which is both streamlined and reliable. The mode-selection involves the tilt control of cavity mirrors and the radius control of the circular aperture in favor of the donut-shaped LG_{01} mode over others due to their different sensitivity to the resonator misalignment. By tuning the angle of the insert fused silica plate, nanosecond lasers in $LG_{0,+1}$, and $LG_{0,-1}$ modes are directly obtained with average power of 22.77 W and 21.85 W, and their pulse energies are 4.55 mJ and 4.37 mJ, respectively. The approach in this paper provides a concise solution for creating high-power vortex laser with slab resonator. Its potential for further power scaling holds promises for diverse applications, extending beyond industry manufacturing to fields like remote sensing, medical treatment, precision measurement, and scientific research.

1 Introduction

Optical vortex laser, with donut-like intensity distribution and whirlpool-like phase distribution, have been widely used in optical communication [1–3], optical tweezers [4–6], material processing [7, 8] and many other fields. Since Couillet et al. first proposed the concept of optical vortex based on Maxwell-Bloch Eq. [9], optical vortex laser with orbital angular momentum (OAM) of $\pm \hbar$ per photon has been studied by several research teams.

A typical optical vortex laser is Laguerre-Gaussian (LG_{pl}) mode, where $p=0$. The generation of LG_{pl} beams can be realized by using specific optical components such as spiral phase plate [10], spatial light modulator [11], and computer-generated holographic converter [12]. Considering the price of components and the complexity of the system,

relatively simple methods have been adopted, such as using annular pump [13, 14] and using astigmatic mode converter (AMC) to convert the diagonally arranged Hermite-Gaussian (HG_{mn}) mode generated by off-axis diode pumped solid state laser to LG_{pl} mode [15–17].

Due to the increasing application scenarios, the generation of vortex laser beams with both tens of watts average power and millijoule level single pulse energy is becoming a hot topic. However, only few works for vortex laser beams have been reported with average powers more than ten-watt level, also most single pulse energy were less than 1 mJ. For instance, a 16.6 W average power LG_{01} mode at 150 kHz was generated in a stigmatic Nd: YVO₄ bounce oscillator. But the single pulse energy was only 0.1 mJ. While the beam quality factors in the x and y axis were $M_x^2 = 1.7$ and $M_y^2 = 1.9$, respectively. The M^2 were less than the theoretical value of 2 for a pure LG_{01} mode, suggesting the presence of some power in the fundamental mode [18]. In another work, a 31.3 W average power vortex laser beam with a beam quality factor M^2 of 2.25 had been achieved by using an imbalanced Sagnac interferometer as output coupler (OC), while the single pulse energy was only 303 μJ [19]. Recently, a 1.51 mJ pulsed $LG_{0,-1}$ mode at 2 μm from a annular pump Tm: LuYAG laser was reported. Unfortunately, their average power was less than 1 W [14]. These solutions still require relatively complex precision devices and delicate optical path design, and laser rod is often used

✉ Jing Yang
yangjing@mail.ipc.ac.cn

¹ Key Lab of Solid State Laser, Technical Institute of Physics and Chemistry, Chinese Academy of Sciences, Beijing 100190, China

² University of Chinese Academy of Sciences, Beijing 100190, China

³ Beijing Institute of Tracking and Communication Technology, Beijing 100094, China

as the gain medium so that the output power is slightly limited. According to our previous work, slabs have been widely used in high-power laser systems because of their large gain volume, great pump uniformity, and favorable thermal management [20], which also make it an expected method for direct generation of optical vortex laser.

In this paper, a new method for direct generation of high average power and millijoule level single pulse energy optical vortex laser via intracavity mode selection in a slab resonator is reported. By controlling the tilt angle of the two cavity mirrors and the radius of the circular aperture, the fundamental mode is suppressed, so that only the LG_{01} mode oscillates in the slab resonator. Compared with other widely used methods, the method proposed in this article is more concise since the LG_{01} mode can be realized by simply inserting a circular aperture and a phase plate in the laser cavity. Here, a laser diode array (LDA) surface-pumped Nd:YAG slab is employed as gain medium because of its favorable thermal management and high pump level. On the other hand, the LDA pump source operating in the quasi-continue-wave (QCW) format can strongly reduce the thermal load in the gain medium while maintaining a high gain [21]. As a result, a vortex $LG_{0,+1}$ mode laser with 22.77 W average power is directly obtained, operating at 50 kHz Q-switching repetition rate and 500 Hz pump pulse repetition rate (PRR) with 250 μ s pump pulse duration. The output is a train contains 10 pulses in each envelope and accordingly 5000 pulses are generated per second with 122 ns pulse width, corresponding to a record 4.55 mJ single pulse energy and a 37.33 kW peak power. In addition, 21.85 W $LG_{0,-1}$ mode laser is also be generated, corresponding to a single pulse energy of 4.37 mJ. By Further increasing the size of the slab and pump module, power scaling of the optical vortex laser can be expected.

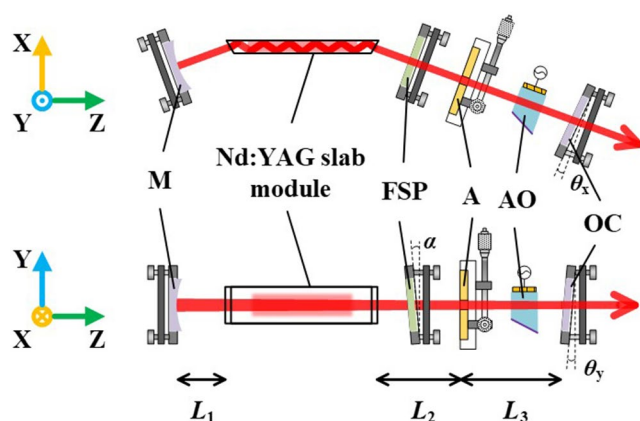


Fig. 1 Experimental setup of the mode-selection slab resonator for generating optical vortex laser. M: rear cavity mirror, FSP: fused silica plate, A1: circular aperture, AO: acousto-optic Q-switch, OC: output coupler

2 Experimental setup

The experimental setup of the Nd:YAG mode-selection slab resonator for generating high-power vortex LG_{01} mode beam is shown in Fig. 1, including a slab laser module, a circular aperture A1, a rear cavity mirror M, a OC, a fused silica plate (FSP), and an acousto-optic (AO) Q-switch. The home-made laser module contains a 0.6 at% doped Nd:YAG slab crystal with dimensions of 139 mm \times 20 mm \times 4 mm (length \times width \times thickness) is used in this experiment. The cut angle of the two end faces of the slab is 56° and both are coated with anti-reflective (AR) film at 1064 nm. The top surface of the slab is coated with an AR film at 808 nm, and the bottom surface of the slab is highly reflective (HR) at 808 nm for a double-pass pumping. The top surface of the slab is edge sealed with an O-ring, while the bottom surface is soldered on the oxygen free copper heat sink with a microchannel cooler, in order to maintain the temperature of the gain module, 20 $^\circ$ C (± 0.2 $^\circ$ C) water with 10 L/min is flow through the cooler and the top surface of the slab. The 808 nm QCW pump.

beam is normally incident on the top surface of the slab via a quartz duct. The pump source consists of 2 LDAs, each array containing 6 bars, providing a total pump power of 560 W with 250 μ s pulse duration and 500 Hz pulse repetition rate (PRR). The laser beam propagates along zig-zag path in the slab. Rear cavity mirror M is a concave mirror with curvature radius R_1 of 2400 mm coated with HR at 1064 nm. The OC with a transmittance of 40% is placed on a rotating stage with finely adjustable tilt angle. A 6 mm-thick FSP is used as a chirality controller, which can cause the output laser to exhibit two opposite helical wavefronts by adjusting its deflection angle on the y-o-z plane [13]. Both sides of the FSP are AR coated at 1064 nm to reduce the insertion loss, and the high damage threshold fused silica also guarantee its power tolerance. The arm lengths from the end facets of the slab to M and OC are $L_1 = 140$ mm and $L_2 = 720$ mm, respectively. The circular aperture A1 is placed at a distance L_3 of 220 mm from OC. The AO Q-switch is located between the circular aperture and OC.

As mentioned above, the diameter of the circular aperture should be selected based on the resonator. Since the zig-zag optical path in the slab averages the thermal gradient, the first-order thermal lens effect is almost ignored. The diameter of the beam at the position of the circular aperture can be calculated by the ABCD propagation matrix, which is given by

$$\begin{pmatrix} A & B \\ C & D \end{pmatrix} = \begin{pmatrix} 1 & L_s + L_1 + L_2 \\ 0 & 1 \end{pmatrix} \begin{pmatrix} 1 & 0 \\ -\frac{2}{R_1} & 1 \end{pmatrix}$$

$$\begin{aligned} &\times \begin{pmatrix} 1 & L_s + L_1 + L_2 \\ 0 & 1 \end{pmatrix} \begin{pmatrix} 1 & L_3 - L_Q + \frac{L_Q}{n_q} \\ 0 & 1 \end{pmatrix} \\ &\times \begin{pmatrix} 1 & 0 \\ -\frac{2}{R_2} & 1 \end{pmatrix} \begin{pmatrix} 1 & L_3 - L_Q + \frac{L_Q}{n_q} \\ 0 & 1 \end{pmatrix}, \end{aligned} \tag{1}$$

where $L_s = \frac{L}{n \cos(\beta)}$ is the optical path length in the slab, L is the length of the Nd: YAG slab, n is the refractive index of Nd: YAG which is 1.82, β is the angle between the laser path and the bottom surface of the slab, L_Q is the length of the AO Q-switch which is 50 mm, n_q is the refractive index of the AO Q-switch which is 1.45, R_2 is the curvature radius of OC, which is taken as positive infinity in calculation. With the laser system presented in Fig. 1, the beam diameter under the assumption of fundamental mode can be expressed by

$$d_0 = 2 \left(\frac{\lambda}{\pi} \right)^{\frac{1}{2}} |B|^{1/2} \left[1 - \left(\frac{D + A}{2} \right)^2 \right]^{-1/4}, \tag{2}$$

where λ is the wavelength of the oscillating laser. Considering the beam diameter ratio between LG_{pl} mode and fundamental mode $d_{pl} = \sqrt{2p + l + 1} d_0$ in cylindrical coordinates [22], for a calculated 1.28 mm diameter fundamental mode here, the corresponding beam diameter of LG_{01} mode is about 1.81 mm. Because of the better mode selection effect when the aperture diameter is slightly larger than the beam diameter in the experiment, the diameter of the circular aperture is selected to be 2.3 mm.

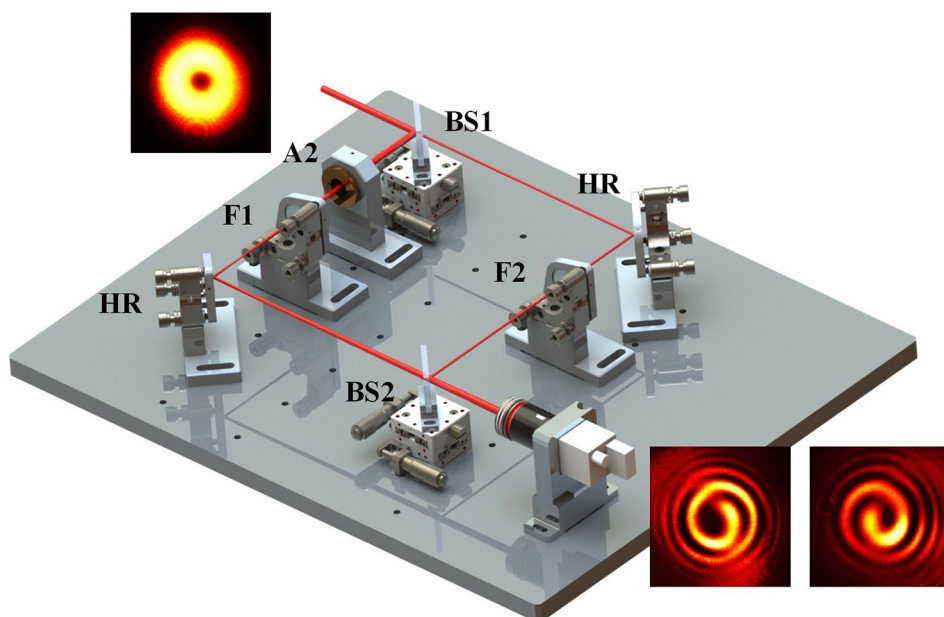
3 Results and discussion

A CMOS camera (CMOS-1201EL, CINOGY Inc.) is used to measure the intensity distribution of the output laser. By adjusting the OC tilt angle, the intensity distribution of the output beam is changed accordingly and monitored by the CMOS. It is found that when the tilt angle θ_x and θ_y are both set around 10 μ rad, the fundamental mode is effectively suppressed. After that, the deflection angle of the FSP is adjusted to change the chirality of the output laser, so that the vortex LG_{01} mode laser beam with the strongest contrast of spatial profile is displayed on the CMOS. The typical two-dimensional (2D) intensity distribution of the output LG_{01} mode laser is shown in the upper left inset of Fig. 2.

In order to verify the vortex property of the output laser beam, an interference experiment of the LG_{01} mode laser beam and a reference beam with spherical wavefront is performed with a homemade Mach-Zehnder (MZ) interferometer to characterize the spatial phase of the output laser beam. The beam profile after interference is also recorded by the CMOS camera. The schematic diagram of the interferometer is shown in Fig. 2. Two typical interference patterns of the output laser beams are displayed when the tilt angles of FSP are adjusted to -2.5° and 2.8° respectively, as shown in the right insets of Fig. 2. These patterns indicate that two LG_{01} modes with clear spiral structures can be oscillated by this resonator: one is left-handedness, and the other is right-handedness, corresponding to the $LG_{0,+1}$ mode and $LG_{0,-1}$ mode, respectively.

In order to obtain nanosecond optical vortex with higher average power, the repetition rate of Q-switching needs to be optimized. The output power of the generated $LG_{0,+1}$ and $LG_{0,-1}$ mode laser at different Q-switching repetition

Fig. 2 Schematic diagram of the homemade Mach-Zehnder interferometer. Inset: typical intensity distribution of the optical vortex laser and the corresponding interference patterns with $LG_{0,+1}$ mode and $LG_{0,-1}$ mode



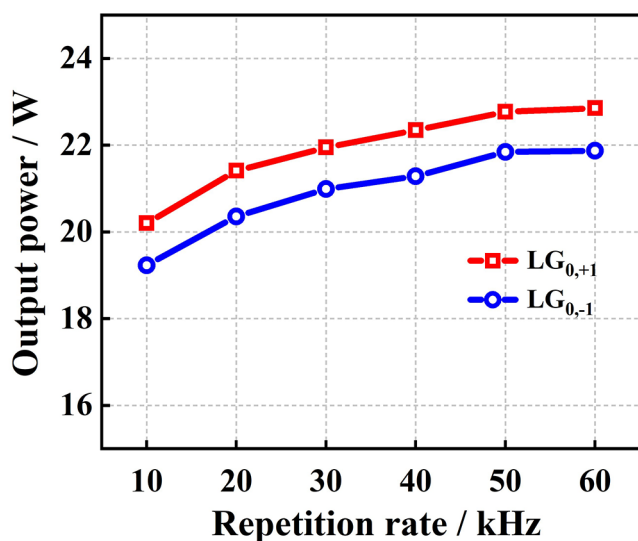


Fig. 3 Output power of $LG_{0,-1}$ mode and $LG_{0,+1}$ mode laser at different Q-switching repetition rate

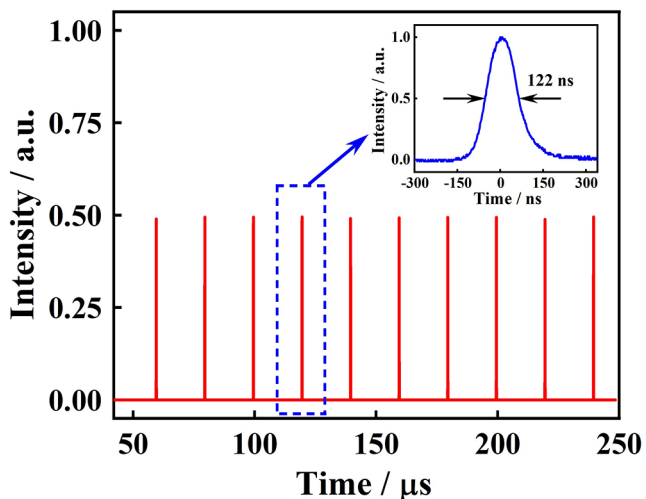


Fig. 4 Oscilloscope traces of the pulse train. Inset: expanded profile of a single pulse

rate under 414.5 W absorbed pump power is measured respectively with a power meter (30A-BB-18, Ophir Inc.), as shown in Fig. 3. It can be seen that there is a significant rise in average power as the repetition rate increases from 10 kHz to 50 kHz.

Meanwhile, the pulse temporal characteristics of the output laser at different Q-switching repetition rate is monitored by a photodiode detector (DET10N/M, Thorlabs Inc.) connected to a 300 MHz bandwidth digital oscilloscope (SDS1204X-E, SIGLENT Inc.). As the repetition rate rises to 60 kHz and beyond, the fluctuation between pulses within the pulse train becomes pronounced, leading to a swift degradation in the stability of the pulses. This is because the population inversion is limited corresponding to a given pump rate, which prevents the oscillator from

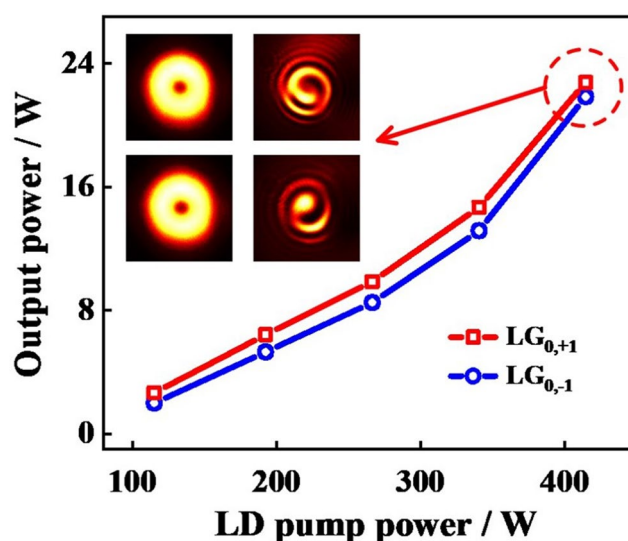


Fig. 5 $LG_{0,-1}$ mode and $LG_{0,+1}$ mode output power of the Nd:YAG slab laser versus pump power. Inset: typical 2D intensity distributions and corresponding interference patterns of the output $LG_{0,+1}$ and $LG_{0,-1}$ mode laser beams

operating at 60 kHz or higher repetition rate [23]. Figure 4 shows a typical pulse train of $LG_{0,+1}$ mode laser output at 50 kHz Q-switching repetition rate. It is found there are 10 nanosecond pulses in each 250 μ s pump pulse envelope, and the Q-switch operates at a PRR of 50 kHz. Considering the pump source operates at 500 Hz PRR, 5000 pulses are generated per second. The pulse-to-pulse fluctuation in the pulse train is less than 2.8% (Std Dev). The inset of Fig. 4 expresses a typical expanded single pulse profile, showing a pulse width of 122 ns. Therefore, considering the average power and temporal fluctuation, the repetition rate of Q-switching is fixed at 50 kHz.

Figure 5 shows the average output power versus the LD pump power in Q-switching operation at 50 kHz, where the red square represents $LG_{0,+1}$ mode and the blue circle represents $LG_{0,-1}$ mode. The intensity distributions and the corresponding interference patterns of the $LG_{0,+1}$ and $LG_{0,-1}$ mode laser beams at the maximum output power are also shown in the insets of Fig. 5. The LD pump thresholds are about 60 W and 62 W for $LG_{0,+1}$ mode and $LG_{0,-1}$ mode, respectively. It can be seen from Fig. 5 that the output power of both modes increases monotonously with the incident pump power and their output power does not show any saturation effect up to around 415 W absorbed pump power. For the $LG_{0,+1}$ mode, a maximum output power of 22.77 W is obtained at 414.5 W absorbed pump power, corresponding to an optical-to-optical efficiency of 5.49%. Considering the output of 5000 pulses per second and the pulse width of 122 ns, the corresponding single pulse energy of $LG_{0,+1}$ mode is 4.55 mJ, which is 2 times higher than previous results [14], and the peak power of the $LG_{0,+1}$ mode is up

to 37.33 kW. For the $LG_{0,-1}$ mode, the maximum output power is 21.85 W, the corresponding single pulse energy is 4.37 mJ and the optical-to-optical efficiency is 5.27%. The insertion of the circular aperture is the main reason for the low optical-to-optical efficiency, the average power is only about 20% of the scheme without circular aperture. In addition, the slight misalignment of the cavity also results in the low optical-to-optical efficiency.

Meanwhile, the power stability is measured at the maximum output power of the $LG_{0,+1}$ mode, as shown in Fig. 6. The relative deviation of the power fluctuation is less than $\pm 1.5\%$ over 30 min, and the corresponding standard deviation is less than 0.6%. The power stability of the $LG_{0,-1}$ mode at the maximum output power is also less than 0.7% (Sta Dev). Clear spiral structures with right-handedness and left-handedness still be observed after about thirty minutes, indicating that the mode-selection based on mirror misalignment and FSP insertion is effective, and this slab resonator is a stable and reliable setup.

The slight tilt control of the cavity and the insertion of the FSP are the two keys for the oscillation of $LG_{0,+1}$ and $LG_{0,-1}$ modes. Previous studies have shown that for a given resonator structure, slight misalignment of the cavity introduces higher loss to the low-order modes [24], so that high-purity one-dimensional HG_{n0} and HG_{0n} modes can be obtained by adjusting the OC tilt angle [25]. In this experiment, the lower order LG_{00} mode is suppressed by adjusting the OC tilt angle θ_x and θ_y to about 10 μrad simultaneously,

Fig. 7 Optical spectra of $LG_{0,+1}$ mode, $LG_{0,-1}$ mode, and the disordered state. Inset: typical 2D intensity distribution of the disordered state

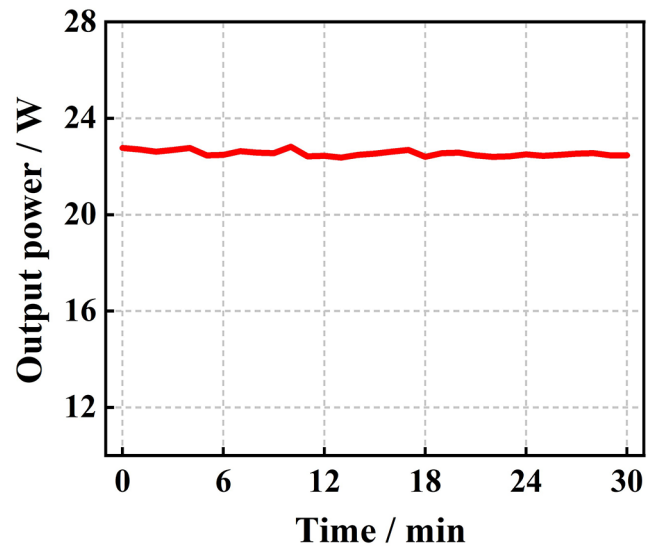
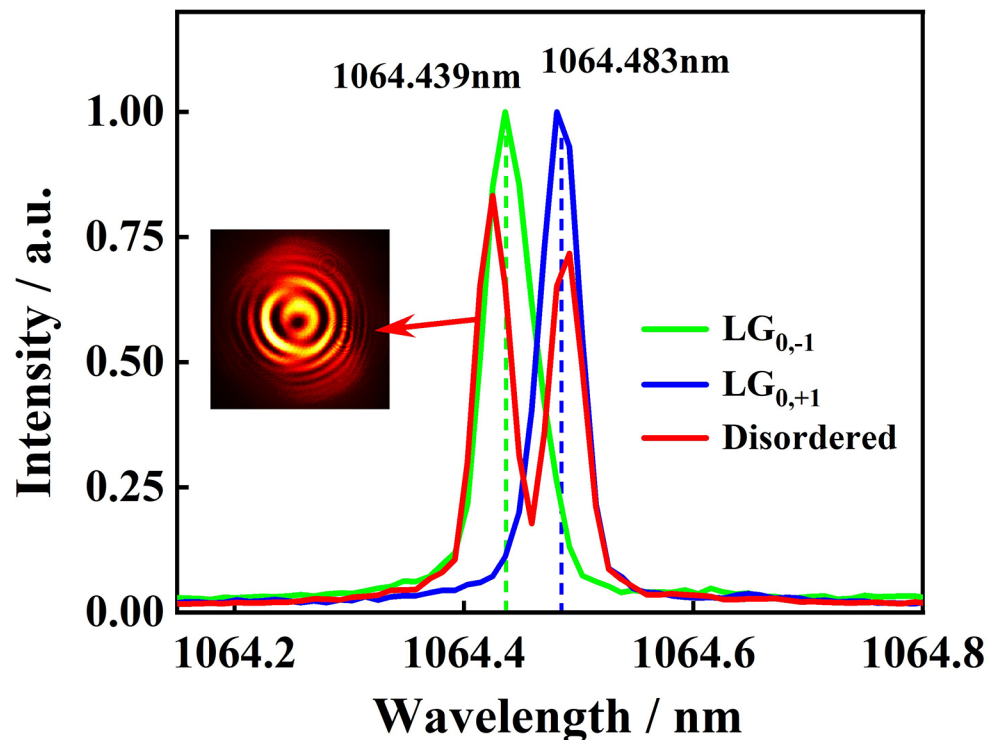


Fig. 6 Power stability of $LG_{0,+1}$ mode at maximum output power over 30 min

so that only the LG_{01} mode oscillates in the circular aperture resonant cavity.

The FSP is another key to the oscillation. The tilted FSP resulting in different cavity loss for each helical-wavefront beam, distinguishing the two opposite helical wavefronts, allowing the selection of handedness in the oscillator. In another word, the FSP and etalon have similar function [13, 26]. The optical spectra of the output lasers are measured with a high-resolution (0.04 nm) optical spectrum analyzers (SHR, Solar laser Inc.), and the results are shown in Fig. 7.

It can be seen the optical spectrum of the $LG_{0,+1}$ and $LG_{0,-1}$ modes are centered at 1064.483 nm and 1064.439 nm, and the corresponding full width at half maximum (FWHM) are 0.043 nm and 0.05 nm, respectively. The narrow emission spectrum also indicates that FSP plays a role similar to that of an etalon. When the FSP is placed perpendicularly to the propagating direction, i.e. $\alpha \approx 0^\circ$, it cannot introduce asymmetric cavity loss between the two LG_{01} modes with opposite helicity, so that the output beam is a “mixed” disordered state without well-defined handedness and there are two peaks in the optical spectra. The typical interference pattern of the disordered mode is shown in the inset of Fig. 7, which is very different from the patterns shown in the insets of Fig. 5.

4 Conclusion

In summary, we propose and demonstrate an approach to directly generate optical vortex laser with high average power and millijoule pulse energy via intracavity mode selection in a slab resonator. By introducing a circular aperture and a fused silica plate in the laser cavity, as well as optimizing the OC tilt angle, the mode selection is realized, achieving the generation of vortex LG_{01} mode laser beam. Without additional complex optical components, this laser has good operability and stability. A vortex $LG_{0,+1}$ mode laser with a high average power of 22.77 W and a record 4.55 mJ single pulse energy is obtained. Further power scaling can be achieved by connecting amplification modules. Moreover, this method is not limited in slab gain media, the high-power optical vortex laser also can be obtained in rod gain media and even gas gain media, enabling them to play greater potential in many fields such as industrial processing, military defense, and scientific research.

Author contributions TLY and JY completed most of the manuscript writing and designed laser experiments. TLY and XPL completed the construction of the laser system. HW and ZZZ assisted in optimizing the laser and participated in testing, and YPW and XJW assisted in writing the manuscript. All authors reviewed the manuscript and provided their respective inputs.

Data availability No datasets were generated or analysed during the current study.

Declarations

Competing interests The authors declare no competing interests.

References

1. J. Wang, Advances in communications using optical vortices. *Photon Res.* **4**(5), 14–28 (2016)
2. J.A. Anguita, J. Herreros, I.B. Djordjevic, Coherent Multimode OAM superpositions for Multidimensional Modulation. *IEEE Photo J.* **6**(2), 790081 (2014)
3. J. Wang, J.Y. Yang, I.M. Fazal, N. Ahmed, Y. Yan, H. Huang, Y. Ren, Y. Yue, S. Dolinar, M. Tur, A.E. Willner, Terabit free-space data transmission employing orbital angular momentum multiplexing. *Nat. Photo.* **6**(7), 488–496 (2012)
4. M. Padgett, R. Bowman, Tweezers with a twist. *Nat. Photo.* **5**(6), 343–348 (2011)
5. M. Woerdemann, C. Alpmann, M. Esseling, C. Denz, Advanced optical trapping by complex beam shaping. *Laser Photo Rev.* **7**(6), 839–854 (2013)
6. N.B. Simpson, L. Allen., M.J. Padgett, Optical tweezers and optical spanners with Laguerre-Gaussian modes. *J. Mod. Optic.* **43**(12), 2485–2491 (1996)
7. Z. Luo, C. Wang, X.R. Dong, J.A. Duan, Femtosecond laser highly-efficient plane processing based on an axicon-generated donut-shaped beam. *Chin. Opt. Lett.* **16**(3), 031401 (2018)
8. C. Hnatovsky, V.G. Shvedov, W. Krolikowski, A.V. Rode, Materials Processing with Femtosecond Vortex pulses. *Opt. Lett.* **35**(20), 3417–3419 (2010)
9. P. Couillet, L. Gil, F. Rocca, Optical vortices. *Opt. Commun.* **73**(5), 403–407 (1989)
10. V.V. Kotlyar, A.A. Almazov, S.N. Khonina, V.A. Soifer, Generation of phase singularity through diffracting a plane or gaussian beam by a spiral phase plate. *J. Opt. Soc. Am. A* **22**(5), 849–861 (2005)
11. N. Matsuoto, T. Ando, T. Inoue, Y. Ohtake, N. Fukuchi, T. Hara, Generation of high-quality higher-order Laguerre-gaussian beams using liquid-crystal-on-silicon spatial light modulators. *J. Opt. Soc. Am. A* **25**(7), 1642–1651 (2008)
12. N.R. Heckenberg, R. McDuff, C.P. Smith, A.G. White, Generation of optical phase singularities by computer-generated holograms. *Opt. Lett.* **17**(3), 221–223 (1992)
13. Y.G. Zhao, Q.Y. Liu, W. Zhou, D.Y. Shen, ~1 mJ pulsed vortex laser at 1645 nm with well-defined helicity. *Opt. Express.* **24**(14), 15596–15602 (2016)
14. Y. Chen, M.M. Ding, J.L. Wang, L. Wang, Q.Y. Liu, Y.G. Zhao, Y. Liu, D.Y. Shen, Z.P. Wang, X.G. Xu, V. Petrov, High-energy 2 um pulsed vortex beam excitation from a Q-switched tm:LuYAG laser. *Opt. Lett.* **45**(3), 722–725 (2020)
15. Y.J. Shen, Y. Meng, X. Fu, M.L. Gong, Wavelength-tunable hermite-gaussian modes and an orbital-angular-momentum-tunable vortex beam in a dual-off-axis pumped Yb:CALGO laser. *Opt. Lett.* **43**(2), 291–294 (2018)
16. S.C. Chu, T. Ohtomo, K. Otsuka, Generation of doughnutlike vortex beam with tunable orbital angular momentum from lasers with controlled hermite-gaussian modes. *Appl. Opt.* **47**(14), 2583–2591 (2008)
17. Y.J. Shen, Y. Meng, X. Fu, M.L. Gong, Dual-wavelength vortex beam with high stability in a diode-pumped yb:CaGdAlO₄ laser. *Laser Phys. Lett.* **15**(5), 055803 (2015)
18. S.P. Chard, P.C. Shardlow, M.J. Damzen, High-power non-astigmatic TEM₀₀ and vortex mode generation in a compact bounce laser design. *Appl. Phys. B* **97**(2), 275–280 (2009)
19. J.W.T. Geberbauer, W.R. Kerridge-Johns, M.J. Damzen, > 30 W vortex LG_{01} or HG_{10} laser using a mode transforming output coupler. *Opt. Express.* **29**(18), 29082–29094 (2021)
20. L. Zhang, Y.D. Guo, Z.Z. Chen, K.L. Gong, J.L. Xu, L. Yuan, Y.Y. Lin, S. Meng, Y. Li, C.F. Shao, S. Li, Z.F. Zhang, Y. Bo, Q.J. Peng, D.F. Cui, Z.Y. Xu, A Near 60% efficiency single-slab nd:YAG High-Power Laser with Adjustable Pulse Duration. *IEEE Photonics Tech. Lett.* **31**(5), 405–408 (2019)
21. Z.X. Song, B.S. Wang, Y. Shen, Y. Bo, J.Q. Chang, Z.Z. Chen, Y.D. Guo, L. Yuan, Y.Y. Lin, Y. Kou, Q. Bian, D.F. Cu, Q.J. Peng,

- QCW surface-pumped cryogenically cooled single-slab laser with 1 kW level at 946 nm. *Appl. Opt.* **61**(10), 2898–2902 (2022)
22. W. Koechner, *Solid-state Laser Engineering* (Springer, New York, 2006)
 23. T.L. Yang, J. Yang, W.Z. Zhou, X.P. Li, X.J. Wang, Q.J. Peng, 100 kHz high power high beam quality nanosecond laser oscillator. *High. Power Laser Part. Beams.* **35**(7), 071006 (2023)
 24. R.J. Freiberg, A.S. Halsted, Properties of Low Order transverse modes in argon ion lasers. *Appl. Opt.* **8**(2), 355–362 (1969)
 25. T.L. Yang, J. Yang, W.Z. Zhou, X.P. Li, Y.N. Zhou, Z.Z. Zhang, X.J. Wang, High-Power, high-purity HG_{0m} hermite–Gaussian Laser Beam Generation in Cascaded large aspect ratio slabs. *Appl. Sci.* **13**(19), 11062 (2023)
 26. D.J. Kim, J.W. Kim, Direct generation of an optical vortex beam in a single-frequency nd:YVO₄ laser. *Opt. Lett.* **40**(3), 399–402 (2015)

Publisher's Note Springer Nature remains neutral with regard to jurisdictional claims in published maps and institutional affiliations.

Springer Nature or its licensor (e.g. a society or other partner) holds exclusive rights to this article under a publishing agreement with the author(s) or other rightsholder(s); author self-archiving of the accepted manuscript version of this article is solely governed by the terms of such publishing agreement and applicable law.